Effect of copper addition on the β-phase formation rate in $FeSi_2$ thermoelectric materials

I. YAMAUCHI, A. SUGANUMA*, T. OKAMOTO, I. OHNAKA
Department of Material Science and Processing, Faculty of Engineering, Osaka University, 2–1, Yamadaoka, Suita, Osaka 565, Japan

The transformation kinetics of the β-phase from an as-solidified structure composed of α and ε in the Fe–Si system was investigated by using rapidly, unidirectionally or conventionally solidified $FeSi_2$ alloys containing a small amount of Cu (0.1–1 at %). The addition of Cu decreased the size of primary ε and slightly changed the solidified eutectic morphology. The solubility of Cu in the α-Fe_2Si_5 phase was estimated to be less than 0.2 at %. A needle-like Cu enriched phase was newly formed in the conventionally solidified alloys containing more than 0.2 at % Cu. Microdifferential thermal analysis (DTA) clearly showed that the addition of Cu drastically accelerated β-phase formation. X-ray diffraction analysis and microstructural observation of the isothermally heat-treated specimens showed that Cu addition was effective in increasing the rate of eutectoid decomposition ($\alpha \rightarrow \beta + Si$) and the initial stage of the peritectoid reaction ($\alpha + \varepsilon \rightarrow \beta$). For complete β formation, heat treatment for a long time was still required because it took a long time for the coarse ε-phase in the slowly solidified alloy to be eliminated by peritectoid reaction. The effect of Cu depended on the annealing temperature. The decomposition rate of α in the Cu-added cast specimen was about 15 times higher at 1073 K than that of the binary cast specimen and exceeded more than 30 times at 873 K.

1. Introduction

β-$FeSi_2$ is known as an excellent high thermoelectric material that can be used in high temperature air atmosphere [1–3]. The equilibrium phase diagram [4] (Fig. 1) shows that an alloy with a stoichiometric composition of $FeSi_2$ will solidify at 1485 K as a eutectic of α-Fe_2Si_5 and ε-phases. However, these high temperature phases are metallic and do not show high thermoelectric power. The β-$FeSi_2$ phase, which shows high thermoelectric power as a semiconductor phase, is formed by the following three reactions:

1. the peritectoid reaction ($\alpha + \varepsilon \rightarrow \beta$) at 1255 K,
2. the decomposition (eutectoid) reaction ($\alpha \rightarrow \beta + Si$) at 1210 K, and
3. the subsequent reaction ($\varepsilon + Si \rightarrow \beta$) [5, 6].

All of these reactions are thermodynamically possible below 1210 K.

A coarse eutectic structure will be formed in the conventional casting process [7, 8] owing to its slow solidification rate. β-phase formation is controlled by diffusion through the solid shell of the β formed by the peritectoid reaction, and hence the reaction rate is slow. It usually takes a long time (more than 100 h) to obtain the full quantity of β for the alloy with a coarse eutectic structure [3, 7]. The β-phase formation rate by eutectoid decomposition is essentially independent of the solidified size of the α structure unlike in peritectoid and subsequent reactions, where a finer structure is preferable to increase the reaction rates. Usually it is difficult to form a fine structure by the conventional casting process. Therefore two processes have been recently attempted to reduce the heat-treatment time. One is to use rapidly solidified powders [7] with a very fine eutectic structure. The other is to use mechanically alloyed powders [9–15]. These processes require powder metallurgy, which causes many problems in producing thermoelectric cells, such as bonding n- and p-type elements. If we can apply a casting process in making thermoelectric cells, the cost will be remarkably decreased.

It was reported that the addition of Cu to β-$FeSi_2$ alloys increased the β-phase formation rate [16]. However, in that paper, Cu powder was added as a binder for sintering and its kinetics details have not been reported. In this paper, we will discuss the effect of Cu on β-phase formation in more detail.

2. Experimental procedure

Binary $FeSi_2$ and various $FeSi_2$–(Cu, Mn, Co) alloys listed in Table I were used. They were prepared from 99.9 mass % electrolytic iron, high purity Si as a semiconductor, 99.9 mass % electrolytic Mn, Co and Cu. They were melted in an aluminium crucible under Ar gas atmosphere. The molten metal was cast into a quartz tube 3 mm in diameter by a vacuum suction

* Present address: Kurimoto Ltd., Kagaya Factory, 1-64, Izumi 2-chome, Suminoe-ku, Osaka 559, Japan.

0022–2461

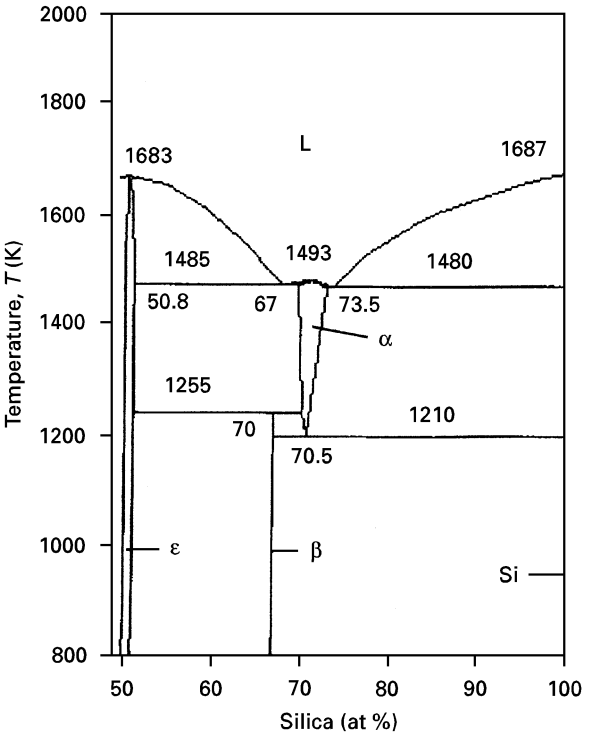

Figure 1 Equilibrium phase diagram of the Fe–Si system (L, liquid).

TABLE I Nominal alloy composition (at %)

Alloy	Fe	Si	Mn	Co	Cu
$FeSi_2$	33.30	66.70	–	–	–
$FeSi_2$–1Cu	32.30	66.70	–	–	1.0
$FeSi_2$–1Mn	32.30	66.70	1.0	–	–
$FeSi_2$–1Co	32.30	66.70	–	1.0	–
$FeSi_2$–1Mn–1Cu	31.30	66.70	1.0	–	1.0
$FeSi_2$–1Co–1Cu	31.30	66.70	–	1.0	1.0
$FeSi_2$–0.1Cu	33.25	66.65	–	–	0.1
$FeSi_2$–0.2Cu	33.20	66.60	–	–	0.2
$FeSi_2$–0.5Cu	33.05	66.45	–	–	0.5
$FeSi_2$–1Mn–0.1Cu	32.25	66.65	1.0	–	0.1
$FeSi_2$–1Co–0.1Cu	32.25	66.65	–	1.0	0.1

method. These cast cylindrical materials were used as slowly solidified specimens. Some specimens of binary $FeSi_2$ and $(FeSi_2)_{99}$ Cu_1 alloys were unidirectionally solidified using the equipment described in a previous paper [8], and rapidly solidified atomized powders (RWA) of these alloys were also produced using a rotating-water-atomization process [17].

The as-solidified structure was observed by back-scattered electron imaging (BEI) using a scanning electron microscope (SEM) without etching. Cyclic heating and cooling experiments using micro differential thermal analyses (DTA) were carried out between 873 K and 1323 K to examine the transformation behaviour. The heating or cooling rate in DTA was 0.25 K s^{-1}. The measured temperature range included the equilibrium peritectoid and eutectoid reaction temperature [4]. Some specimens were quenched into water from given temperatures during DTA measurement.

Isothermal annealing of the β-phase formed was carried out at various temperatures between 873 and 1173 K for a given period in vacuum atmosphere. The change in structure with heat-treatment was also observed by SEM and X-ray diffraction (XRD). The composition of some phases was measured by electron probe X-ray microanalysis (EPMA).

3. Results and discussion

3.1. Effect of Cu addition on the solidified structure

The β-phase transformation rates in $FeSi_2$ alloy strongly depended on the morphology of the solidified structure, as described previously [6]. Therefore, it is necessary to examine the effect of Cu addition on the solidification morphology first.

Fig. 2a shows a well aligned rod-type eutectic structure composed of ε (white circle) and α (dark matrix) that was obtained at a growth rate of 26 μm s^{-1} in a unidirectionally solidified binary $FeSi_2$ alloy. On the other hand, such a well aligned structure was not formed in $FeSi_2$ alloys with the addition of 1 at % Cu unless the growth rate was below about 4 μm s^{-1}. An example of a well aligned structure is shown in Fig. 2b. This result can be explained by instability of the solidification front owing to the constitutional undercooling of Cu, and it is similar to that in Mn- or Co-doped alloys [8].

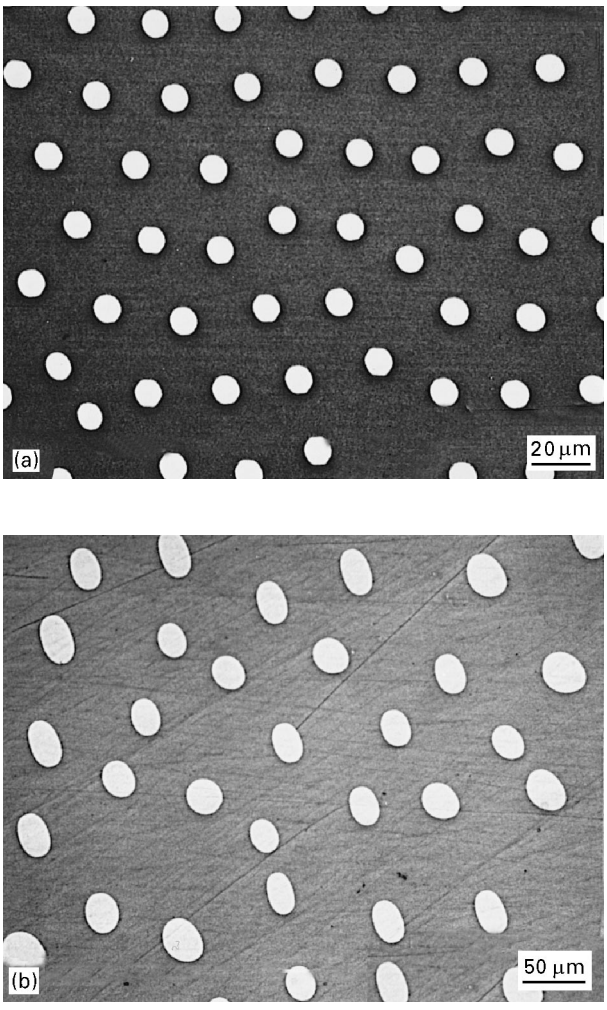

Figure 2 Microstructure of unidirectionally solidified $FeSi_2$ and $FeSi_2$–1Cu alloys (transverse section) : (a) $FeSi_2$ at a growth rate of 26 μm s^{-1}, and (b) $FeSi_2$–1Cu at a growth rate of 4.1 μm s^{-1}.

Fig. 3a–d shows the as-solidified structure of binary and Cu added $FeSi_2$ alloys obtained by the vacuum suction method. The coarse primary dendritic, ε (A in Fig. 3a), and the fine eutectic (B in Fig. 3a) composed of α and ε, were formed in the slowly solidified specimen of binary $FeSi_2$ alloys, though the composition of the alloy was very close to the eutectic composition. On the other hand, it is rather difficult to recognize the typical eutectic structural configuration in the slowly solidified alloy with 1 at % Cu added (Fig. 3b). The difference in morphology between the slowly solidified binary and Cu added $FeSi_2$ alloy was caused by the same mechanism discussed in the unidirectional solidification experiment [8]. A slightly elongated ε (C in Fig. 3b) was formed and also a needle-like phase (D in Fig. 3b) was newly formed. The compositions of the new and other phases were measured by EPMA and the results are summarized in Table II. It was difficult to evaluate the exact content of Cu dissolved in ε and α owing to its low concentration. However, it was obvious that Cu in ε was higher than that in α from the raw EPMA data. Most of the Cu was dissolved in the needle-like phase. The volume fraction of the new phase decreased with decreasing Cu and it disappeared in the alloys below 0.2 at % Cu. These results suggest that the solubility of Cu in α and ε was probably below 0.2 at %.

In the case of rapid solidification, there were no remarkable differences in the structures between the binary and Cu added alloys as shown in Fig. 3c and d. The structures were much finer than those of the slowly solidified specimens. Relatively coarse α was observed as a primary phase and a fine eutectic structure existed in the inter-primary phase region. It was difficult to detect the existence of a Cu-enriched phase in the rapidly solidified Cu-added specimen by SEM observation. Probably, most Cu was dissolved in α or ε by rapid cooling.

The X-ray diffraction patterns of these samples are shown in Fig. 4. Essentially there was no detectable difference among these patterns. All of the as-solidified specimens were composed of α and ε. The quantity of the Cu enriched phase was too low for detection in the slowly solidified Cu added specimen. Also, Fig. 4 does not show any evidence of β-phase formation during solidification.

On the other hand, in the case of an unidirectionally solidified specimen containing Cu, a β + Si phase formed at the bottom part of the specimen as shown in Fig. 5. Such a structure has never been obtained in unidirectionally solidified binary alloys at the same growth condition. In the unidirectional solidification experiment, the sample specimen descended downwards in the furnace [8]. Each part of the unidirectionally solidifying specimen was moved from hotter to lower temperatures. Therefore, the bottom part of the specimen, that means the initially solidified part, was held for a longer period in a temperature range below the eutectoid temperature than the upper part, that means the lately solidified part. The structure shown in Fig. 5 strongly suggested that Cu addition was effective in enhancing β-phase formation.

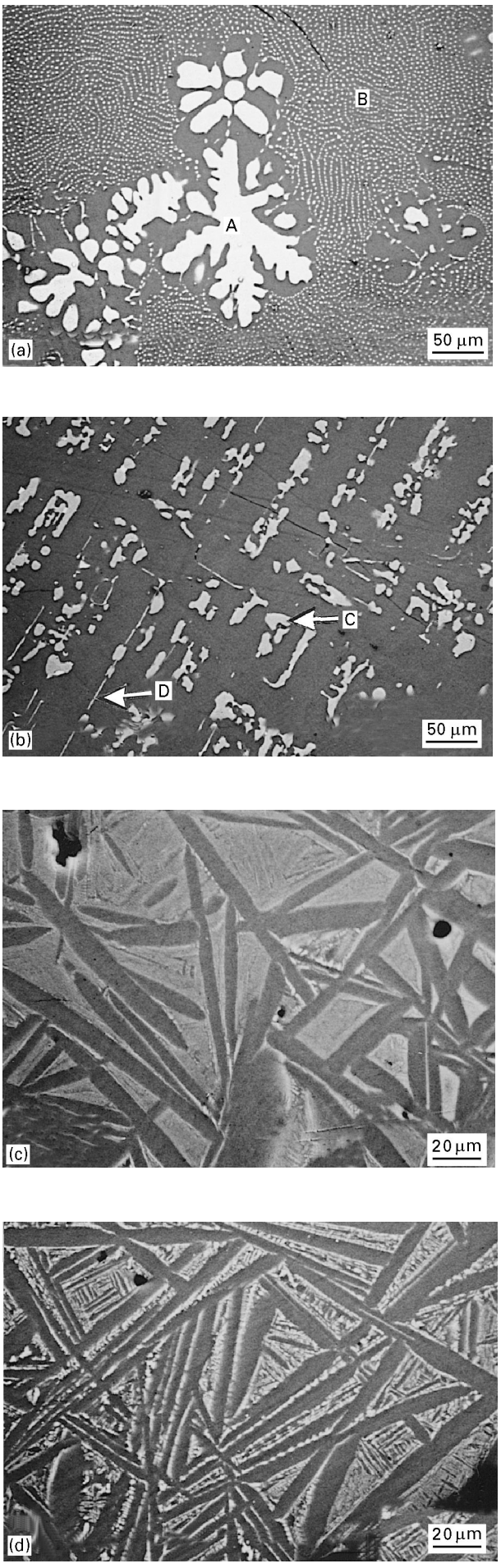

Figure 3 Microstructure of as-solidified $FeSi_2$ and $FeSi_2$–1Cu alloys: (a) $FeSi_2$ slowly solidified, (b) $FeSi_2$–1Cu slowly solidified, (c) $FeSi_2$ rapidly solidified, (d) $FeSi_2$–1Cu rapidly solidified.

TABLE II Results of EPMA analysis of slowly solidified $FeSi_2$–1Cu alloy (mean value, at %)

Phase	Fe	Si	Cu
ε	49.0(± 1)	50.0(± 1)	< 0.5
α	29.0(± 1)	70.0(± 1)	< 0.5
Needle-like	8.4(± 2)	35.4(± 2)	56.2(± 2)

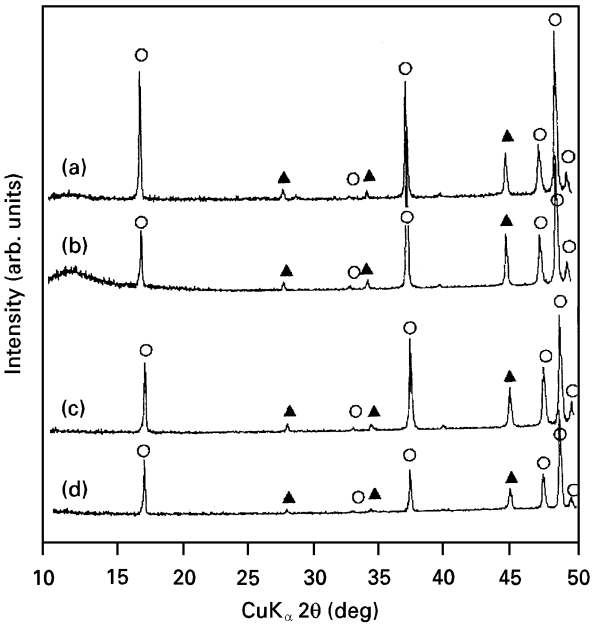

Figure 4 X-ray diffraction patterns of as-solidified (a, b) $FeSi_2$ and (c, d) $FeSi_2$–1Cu alloys produced by rapid (b, d) or conventional slow (a, c) solidification processes: (○) α-phase; (▲) ε-phase.

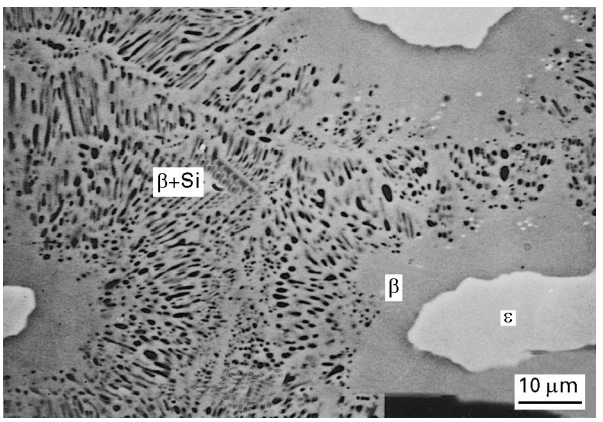

Figure 5 The microstructure at the bottom part of an unidirectionally solidified specimen shows β-phase formation by peritectoid and eutectoid reaction ($FeSi_2$–1Cu; growth rate, 1.1 μm s^{-1}).

3.2. β-phase formation in $FeSi_2$ alloys

To determine the effect of Cu addition on the β-phase formation rate, micro differential thermal analysis (DTA) was carried out for the binary and 1 at % Cu added specimens prepared by the slow and rapid solidification techniques. These results are shown in Fig. 6a–d. Fig. 7a–d shows the X-ray diffraction patterns of the specimens quenched in the various stages during the DTA experiment.

In a slowly solidified binary $FeSi_2$ alloy (Fig. 6a), there was a diffuse exothermic peak during heating stages. One sharp endothermic peak was observed between 1280 and 1300 K. This endothermic reaction temperature corresponded with the equilibrium peritectoid temperature [4]. The X-ray diffraction pattern (Fig. 7a, line A) of the specimen quenched at A in Fig. 6a shows β, α and ε lines and no Si lines. The β-phase was formed by peritectoid reaction with a diffuse exothermic reaction during the heating stage. This β-phase decomposed to α and ε between 1280 and 1300 K with a sharp endothermic reaction. The X-ray diffraction pattern (Fig. 7a, line B) of the specimen quenched at B in Fig. 6a, shows only α and ε and no β nor Si. No detectable reaction occurred during the cooling stage. There are no β and Si lines in the X-ray diffraction pattern (Fig. 7a, line C) of the specimen quenched at C in Fig. 6a. When Cu was added to a binary alloy, DTA curves varied their patterns considerably as shown in Fig. 6b. A large exothermic peak was observed at around 900 K during the first heating stage. The X-ray diffraction pattern (Fig. 7b, line A) of A in Fig. 6b shows β and Si, which were formed by eutectoid or peritectoid reactions, and a few peaks can be attributed to the remaining α-phase. The β and Si phases were decomposed to α with a small endothermic peak. Thus Si lines disappeared as shown in Fig. 7b, line B. Then the remaining β decomposed to α and ε with a large endothermic peak. The X-ray diffraction pattern (Fig. 7b, line C) at C in Fig. 6b shows only α and ε. These phases transformed to β with a sharp exothermic peak during the cooling stage. This peak temperature was remarkably lower than that of the equilibrium temperature and the β-phase transformed with a large undercooling. The degree of the undercooling is an indicator to estimate the qualitative β-phase transformation rate. The transformation rate will decrease with increasing undercooling. The X-ray diffraction pattern (Fig. 7b, line D) at D in Fig. 6b shows β, Si and a few α. The X-ray diffraction pattern (Fig. 7b, line D) at E in Fig. 6b is almost the same as that of D.

The temperature of the second endothermic peak is almost the same as that of the binary alloy (Fig. 6a). The significant differences between the DTA curves (Fig. 6a, b) of the two slowly solidified alloys suggest that the eutectoid decomposition of α to β + Si is much enhanced by the addition of Cu.

The small endothermic reactions at 1090 K in the second and third heating episodes were only observed in Cu added alloys. Therefore the origin of that endothermic reaction will be the decomposition of the Cu enriched phase.

Fig. 6c and d shows DTA curves of the rapidly solidified specimens. In the binary specimen, a sharp exothermic peak was observed in the first heating and two endothermic peaks were also observed. The X-ray diffraction pattern (Fig. 7c, line A) at A in Fig. 6c shows mostly β peaks and a small peak of Si. Therefore, the first exothermic peak was generated from both peritectoid and eutectoid reactions. One of the reasons why the sharp exothermic reaction occurred even in a rapidly solidified binary alloy, may be its

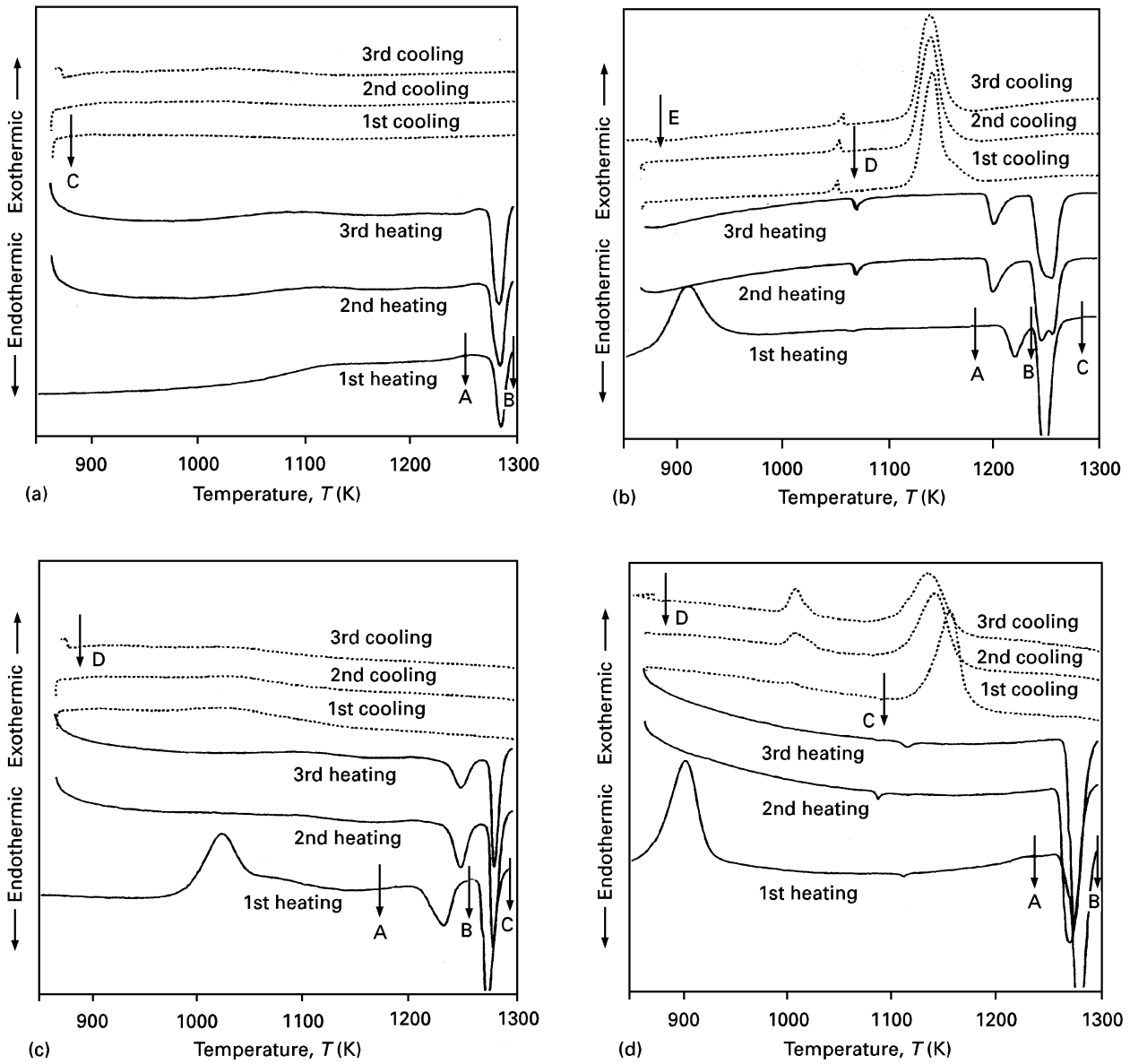

Figure 6 DTA curves of slowly solidified $FeSi_2$ binary (a) and $FeSi_2$–1Cu (b) alloys, and rapidly solidified $FeSi_2$ binary (c) and $FeSi_2$–1Cu alloy (d). (——) on heating, (----) on cooling; numbers refer to first and subsequent episodes of heating/cooling.

quite fine as-solidified structure owing to the rapid cooling. The total surface area contributing to the peritectoid reaction is much increased in the fine structure and it will lead to a sharp exothermic peak meaning higher heat generation as a product of the reacted area and reaction rate per unit area. Two X-ray diffraction patterns (Fig. 7c, lines B and C) at B and C in Fig. 6c show that these two endothermic peaks also arose from eutectoid and peritectoid reactions similar to those in slowly solidified specimens with added Cu. The X-ray diffraction pattern (Fig. 7c, line D) at D in Fig. 6c was almost the same as that of C. There was no significant β-phase formation during cooling. On the other hand, some amount of β-phase formation occurred during heating.

By adding Cu, the first sharp exothermic peak shifted to a lower temperature as shown in Fig. 6d and one endothermic peak existing at lower temperature disappeared. The X-ray diffraction pattern (Fig. 7d, line A) at A in Fig. 6d shows that the structure was almost a single β-phase and it suggested that only peritectoid reaction occurred. It means that peritectoid reaction was also enhanced by Cu addition. As its structure was very fine, β-phase formation by peritectoid reaction finished before the eutectoid reaction started. As a result, peritectoid reaction apparently seemed to be suppressed. This single β-phase decomposed to α and ε at the equilibrium temperature, accompanying an endothermic peak. Therefore the X-ray diffraction pattern (Fig. 7d, line B) at B in Fig. 6d shows no β. Two exothermic peaks were observed in this specimen during the cooling stage. The first large exothermic peak was caused from β-phase formation and it occurred at a lower temperature than that of the equilibrium. The second very small exothermic peak may correspond with the precipitation of a Cu-rich phase, but it is difficult to identify the crystal structure from the X-ray diffraction pattern (Fig. 7d, line D) owing to too small a quantity of the Cu-rich phase.

These results are summarized as follows. In the case of the coarse solidification structure, Cu addition was

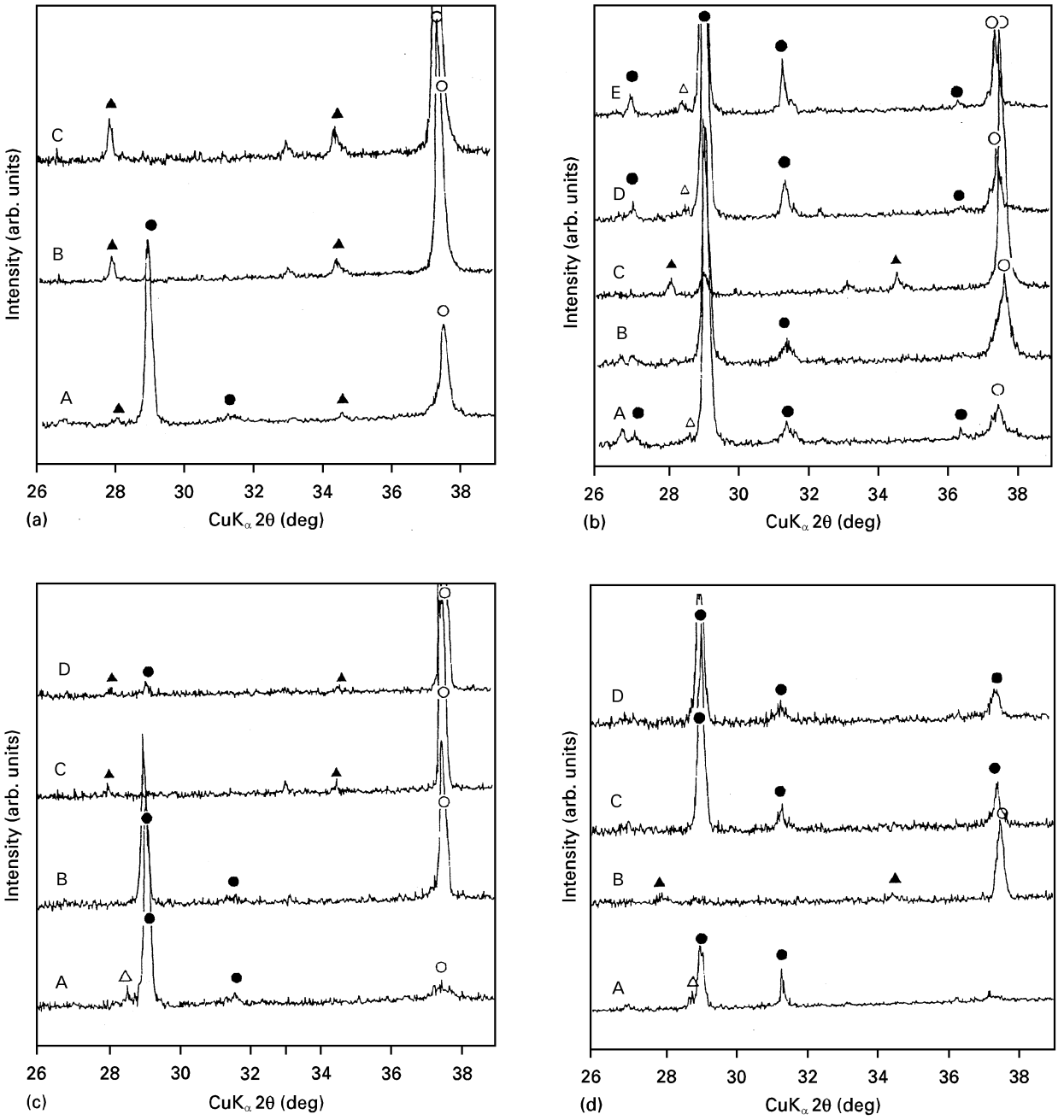

Figure 7 X-ray diffraction patterns of slowly solidified $FeSi_2$ (a) and $FeSi_2$–1Cu (b) alloy and rapidly solidified $FeSi_2$ (c) and $FeSi_2$–1Cu (d) alloy specimens quenched at given various temperatures during DTA measurement: (○) α-phase, (▲) ε-phase, (●) β-phase, (△) Si.

effective in the formation of β by eutectoid reaction. On the other hand, in the fine solidification structure peritectoid reaction will dominate. Schematic illustrations of the effect of Cu addition on the β-phase formation process are shown in Fig. 8a and b. These models were confirmed by heat-treatment of the unidirectionally solidified specimens as shown in Fig. 9a and b. In the binary alloy, no eutectoid reaction was observed (Fig. 9a). On the other hand, eutectoid decomposition was clearly observed with a few peritectoid reactions during a shorter heat-treatment period (Fig. 9b). The solidification structure is usually relatively coarse in conventional casting processes, therefore the eutectoid reaction will be important for β-phase formation.

Fig. 10a and b also clearly shows the effect of Cu on the structure after DTA of the slowly solidified specimens. Sometimes coarse ε was observed even in a Cu added alloy, as shown at A in Fig. 10b. This coarse ε will remain after the long heat-treatment even in a Cu added alloy. Unless the metallic ε-phase was eliminated by the annealing, the thermoelectric power was low and caused an electrical short circuit. To avoid the problem, the basic composition of the alloy should move to Fe_2Si_5 where only the α-phase is formed during solidification, although the final equilibrium phases are β and Si at low temperature.

Fig. 11 shows the effect of Mn or Co, that was added as a dopant, on β-phase formation. The addition of Mn or Co slightly decreased the β-phase formation rate, but the schematic shapes of the DTA curves for the Cu added specimens are almost the same and the effect of Cu is still quite strong.

Quantitative estimation of β-phase formation was obtained by X-ray diffraction of the isothermally heat-treated specimens. Fig. 12 shows an example of the

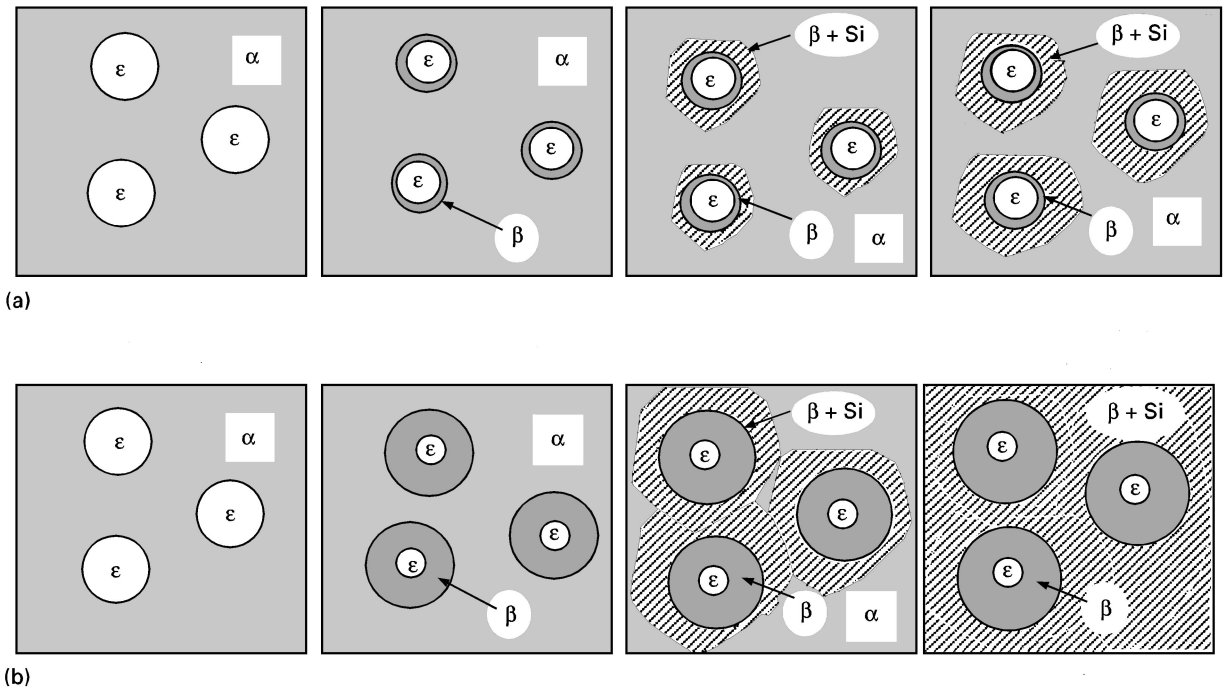

Figure 8 Schematic illustration of the β-phase formation process: (a) $FeSi_2$ binary, and (b) Cu added $FeSi_2$. From left to right: as-solidified; β-phasing by the peritectoid reaction; decomposition of matrix α by the eutectoid reaction; start of the subsequent reaction ($\varepsilon + Si \rightarrow \beta$).

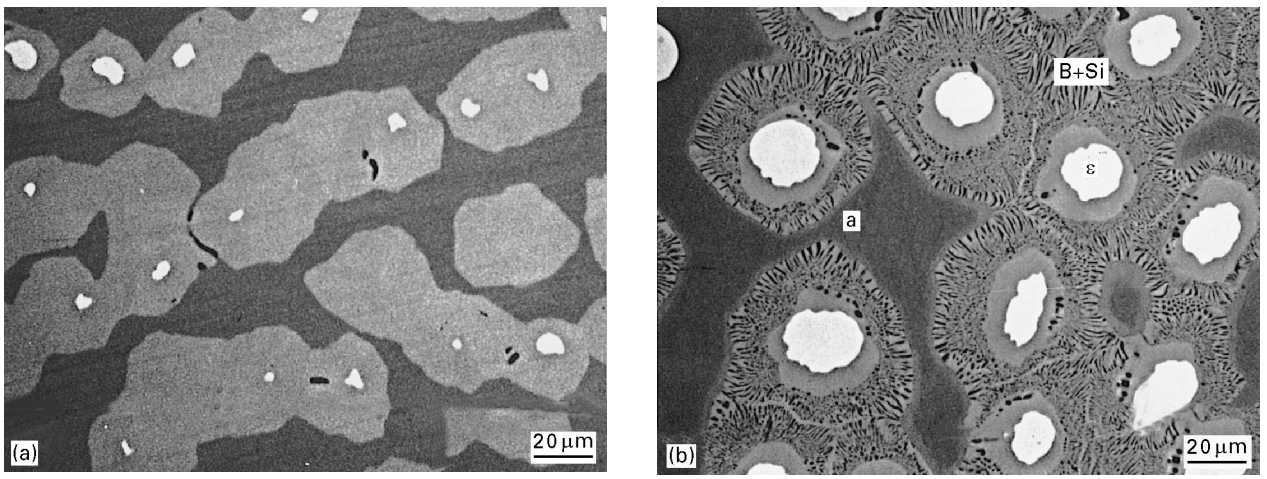

Figure 9 Microstructure of heat-treated samples of unidirectionally solidified $FeSi_2$ and $FeSi_2$–1Cu alloys (1163 K): (a) $FeSi_2$ for 10.8×10^3 s (b) $FeSi_2$–1Cu for 600 s.

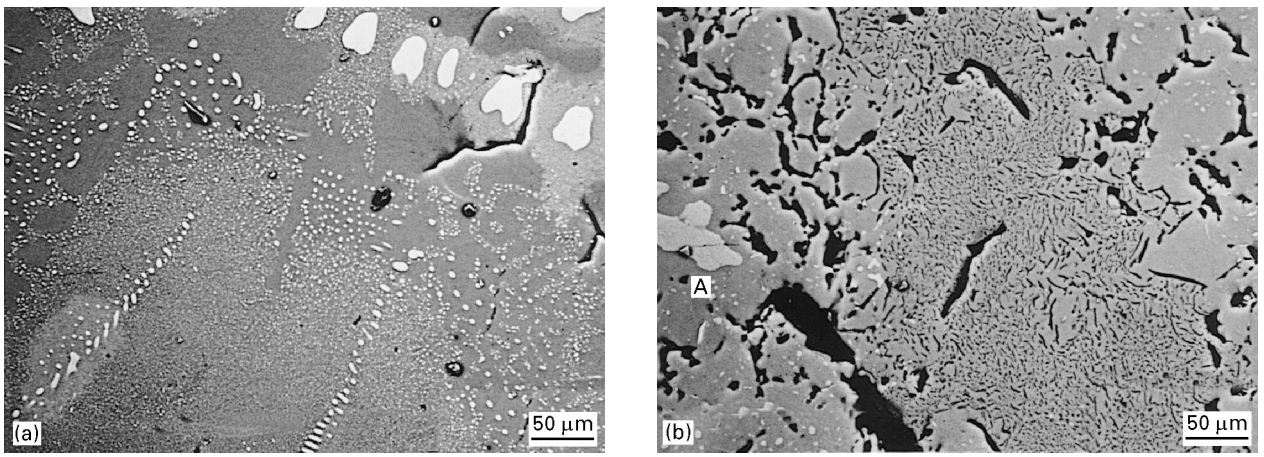

Figure 10 Microstructure of (a) $FeSi_2$ and (b) $FeSi_2$–1Cu slowly solidified specimens.

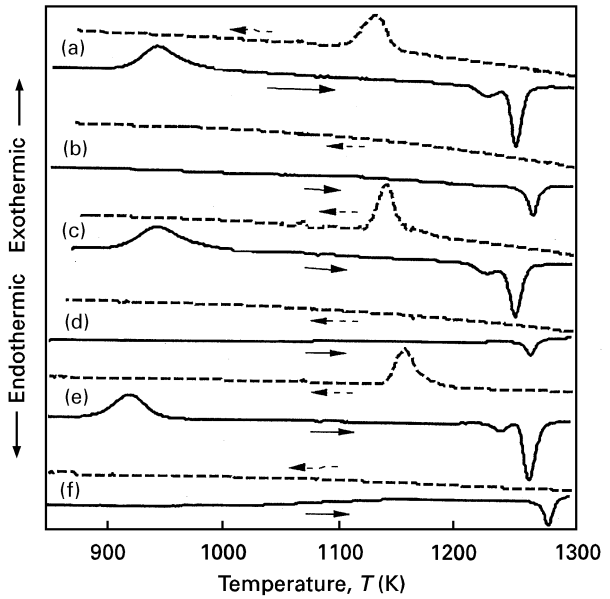

Figure 11 DTA curves for various slowly solidified $FeSi_2$ alloys on cyclic heating (——) and cooling (----) at a rate of $0.25\,K\,s^{-1}$: (a) $FeSi_2$–1Cu–1Co, (b) $FeSi_2$–1Co, (c) $FeSi_2$–1Cu–1Mn, (d) $FeSi_2$–1Mn, (e) $FeSi_2$–1Cu, (f) $FeSi_2$ binary.

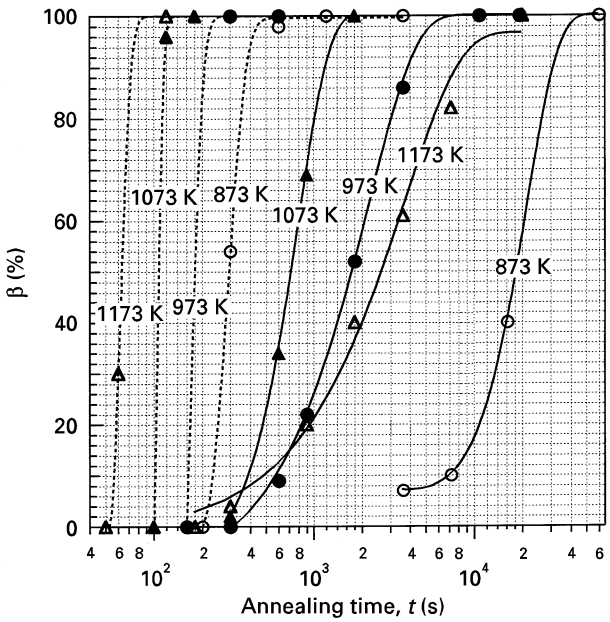

Figure 12 Effects of annealing temperature on β-phase formation in $FeSi_2$ binary (——) and $FeSi_2$–1Cu (----) alloys.

effects of Cu addition and annealing temperature on the β-phase formation in $FeSi_2$ and $FeSi_2$–1Cu alloys. The β-phase formation rate was considerably affected by the annealing temperature. The formation rate of Cu added alloy annealed at 1073 K was about 15 times higher than that of the binary alloy and it exceeded more than 50 times at 873 K. Table III shows the summary of the completely dissolved time of α for various alloys and temperatures. The effects of Cu decreased with decreasing Cu content. It was still six times higher than that of Cu less alloys even in 0.1 at % Cu added alloys annealed at 1073 K. Cu addition in Mn and Co doped alloys also shows similar excellent effects.

TABLE III Summary of elapsed time for 100% β-phase formation (s)

Alloy[a]	Annealing temperature (K)	Time for 100% β (s)
$FeSi_2$	873	6.0×10^4
	973	1.1×10^4
	1073	1.8×10^3
$FeSi_2$–0.1Cu	1073	3.0×10^2
$FeSi_2$–0.2Cu	1073	2.0×10^2
$FeSi_2$–0.5Cu	1073	1.8×10^2
$FeSi_2$–1Cu	873	1.2×10^3
	973	3.0×10^2
	1073	1.2×10^2
	1173	1.2×10^2
$FeSi_2$–1Mn	1073	$>3.6\times10^3$
$FeSi_2$–1Mn–0.1Cu	1073	3.0×10^2
$FeSi_2$–1Mn–1Cu	1073	1.8×10^2
$FeSi_2$–1Co	1073	3.6×10^3
$FeSi_2$–1Co–0.1Cu	1073	3.0×10^2
$FeSi_2$–1Co–1Cu	1073	2.0×10^3

[a] Compositions of additives are measured in at %.

However, these results neglected the existence of ε. Fig. 13 shows the X-ray diffraction patterns of the samples annealed for various periods. In the case of Cu less alloys, peaks of the α-phase almost disappeared in the specimen annealed at 1073 K for 3.6×10^3 s, as shown in Fig. 13a. Sharp ε lines still remained and it was difficult to detect Si lines. These results indicate that peritectoid reaction, where no Si lines may be formed, may be dominant in this alloy. On the other hand, α lines completely disappeared for 3×10^2 s annealing in the 0.1 Cu added alloy, the height of the ε peaks slightly decreased from that of the as-cast state and there is a clear Si peak at $2\theta = 28.5$ corresponding to Si (1 1 1). The Si phase was formed by the decomposition of α by the eutectoid reaction. After the disappearance of α, peaks of ε still remained even at 9.6×10^3 s annealing. These results mean that Cu addition was also effective for shortening of the β formation by the eutectoid decomposition of α as well as by the peritectoid reaction. When a relatively coarse ε phase is formed during solidification, the effect of Cu is reduced. The remaining ε will be harmful for thermoelectric power because it has a metallic phase. Cu addition is also effective in refining the size of ε, but its effect is not so great. Therefore, we will propose a new composition to neglect the existence of ε.

4. Conclusions

1. The solidification morphology was slightly affected by Cu addition. The critical growth rate for a well-aligned rod-type eutectic structure during unidirectional solidification decreased from $26\,\mu m\,s^{-1}$ for the binary alloy to $4\,\mu m\,s^{-1}$ for the 1 at % Cu added alloy.

2. The size of primary dendritic ε in the slowly solidified specimen decreased with Cu addition. Most Cu solidified as a new Cu enriched needle-like phase. The solubility of Cu in the α- and ε-phases was estimated to be less than 0.2 at %.

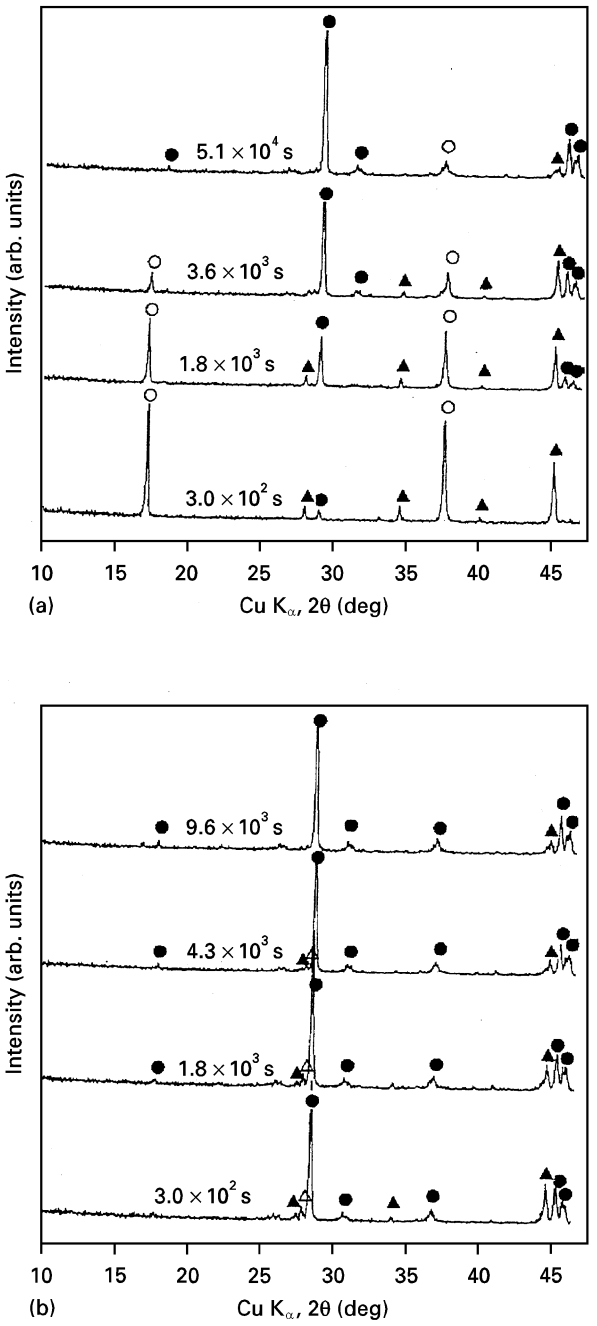

Figure 13 Variation of X-ray diffraction patterns with annealing time shows the effects of Cu addition on β-phase formation in (a) $FeSi_2$–1Mn, and (b) $FeSi_2$–1Mn–0.1Cu at 1073 K. (○) α-phase, (▲) ε-phase, (●) β-phase, (△) Si.

3. The addition of Cu was quite effective in increasing the β-phase transformation rate, especially in the slowly solidified alloys. The eutectoid decomposition of $\alpha \rightarrow \beta + Si$ mostly controlled the transformation rate, although the solubility of Cu in α was quite low.
4. The addition of Mn or Co as a dopant to the Cu added alloys did not significantly decrease the transformation rate.
5. It still took a long time to eliminate the coarse ε-phase because Cu addition was only effective at the initial stage of the peritectoid reaction ($\alpha + \varepsilon \rightarrow \beta$).

References

1. U. BIRKHOLTZ and J. SCHELM, *Fiz. Status. Solidi.* **27** (1968) 413.
2. I. NISHIDA, *Phys. Rev. B* **7** (1973) 2710.
3. T. SAKATA and I. NISHIDA, *Bull. Jpn Inst. Metals* **15** (1976) 1.
4. O. KUBASCHEWSKI, "Iron-binary Phase Diagram" (Springer-Verlag, New York, 1982) p. 136.
5. T. SAKATA, Y. SAKAI, H. YOSHINO, H. FUJII and I. NISHIDA, *J. Less Common Metals* **61** (1978) 301.
6. I. YAMAUCHI, S. UEYAMA and I. OHNAKA, *J. Mater. Sci. Eng.* **15** (1996) 101.
7. I. YAMAUCHI, I. OHNAKA and S. UEYAMA, in Proceedings of the Twelth International Conference on Thermoelectrics edited by K. Matsura (Yokohama, Japan 1993) p. 289.
8. I. YAMAUCHI, S. UEYAMA and I. OHNAKA, *J. Mater. Sci. Eng.* **15** (1996) 108.
9. M. UMEMOTO, *Mater. Trans. JIM* **36** (1995) 373.
10. H. NAGAI, *ibid.* **36** (1995) 365.
11. H. NAGAI, S. IIDA, I. MAEDA, S. KATSUYAMA and K. MAJIMA, *J. Jpn. Soc. Powder & Powder Metall.* **40** (1993) 332.
12. H. NAGAI, I. MAEDA, S. KATSUYAMA and K. MAJIMA, *ibid.* **41** (1994) 560.
13. H. NAGAI, I. NAKAYAMA, S. KATSUYAMA and K. MAJIMA, *ibid.* **42** (1995) 151.
14. S. SHIGA, M. UMEMOTO and I. OKANE, *ibid.* **42** (1995) 141.
15. M. UMEMOTO, *ibid.* **42** (1995) 135.
16. T. TAKEDA and M. KATO, Proceedings of fall meeting of Japanese Society of Powder and Powder Metallurgy, vol. 11 (Nagaya, Japan, 1995) p. 192.
17. I. OHNAKA, T. FUKUSAKO and K. TSUTSUMI, *J. Jpn Inst. Metals* **46** (1982) 1095.

Received 24 June 1996
and accepted 10 February 1997